Journal of Alloys and Compounds 689 (2016) 885–893

Contents lists available at ScienceDirect

Journal of Alloys and Compounds

journal homepage: http://www.elsevier.com/locate/jalcom

Theoretical investigation of the structural, electronic, magnetic and elastic properties of binary cubic C15-Laves phases TbX_2 (X = Co and Fe)

A. Bentouaf [a, b, *], R. Mebsout [c], H. Rached [b, d], S. Amari [b, c], A.H. Reshak [e, f], B. Aïssa [g, h]

[a] Laboratory of Physico-Chemitry of Advanced Materials, University Djillali Liabès, Sidi Bel-Abbes, Algeria
[b] Physics Department, Faculty of Sciences, University of Hassiba Ben Bouali, 02000, Chlef, Algeria
[c] Laboratory of Simulation and Modelisation of Materials, University Djillali Liabès, Sidi Bel-Abbes, Algeria
[d] Laboratory of Magnetic Materials, University Djillali Liabès, Sidi Bel-Abbes, Algeria
[e] New Technologies - Research Centre, University of West Bohemia, Univerzitni 8, 306 14 Pilsen, Czech Republic
[f] Center of Excellence Geopolymer and Green Technology, School of Material Engineering, University Malaysia Perlis, 01007 Kangar, Perlis, Malaysia
[g] Qatar Environment and Energy Research Institute (QEERI), Hamad Bin Khalifa University, Qatar-Foundation, P.O. Box 5825, Doha, Qatar
[h] Centre Energie, Matériaux et Télécommunications, INRS, 1650, Boulevard Lionel-Boulet Varennes, Québec, J3X 1S2, Canada

ARTICLE INFO

Article history:
Received 16 March 2016
Received in revised form
3 August 2016
Accepted 5 August 2016
Available online 7 August 2016

Keywords:
Binary Laves phases
Intermetallic compound
Density of states
GGA
Magnetic properties
Elastic properties

ABSTRACT

We report on a comprehensive theoretical investigation of the physical properties of the cubic $MgCu_2$-type binary Laves phases $TbCo_2$ and $TbFe_2$ compounds. The density functional full-potential linearized augmented planewave (FP-LAPW) method was used. We adopted the generalized gradient approximation (GGA) to estimate the exchange correlation potential and the GGA+U (i.e. Hubbard correction) calculations in accurately characterizing the correlation effects. The lattice parameter a_0, bulk modulus B and magnetic moment M at the equilibrium state were found to well corroborate the experimental data. We have calculated the magnetic moments of Co and Fe in the $TbCo_2$ and $TbFe_2$, respectively, by using GGA and GGA+U methods, where the magnetic moments value of Fe was found to be higher than that of Co. The GGA+U gave higher value than that obtained by GGA. To obtain further insight into the type of states associated with each orbital, the projected density of states of the Co-3d and Fe-3d orbitals were calculated using GGA and GGA+U, respectively. This work highlights the role of the correlated electrons processing for an accurate description of these binary Laves phases compounds.

1. Introduction

The cubic Laves phase compounds RX_2 (R = rare earth, X = transition metal) have been one of highly interesting subjects in solid state physics since the nineteen sixty years due to the metamagnetic RX_2 transition owing to the instability of the metal transition moment [1–5]. Among the various intermetallic compounds of rare-earths with transition-metals, the RX_2 binary Laves phase alloys with ferromagnetic X (Fe and Co) have been particularly attractive both for fundamental investigation of their physical properties -including their electronic structure, the high Curie temperature-, then for their technological applications potential.

Generally, RX_2 (X = Co and Fe) compounds demonstrate the so-called "itinerant electron metamagnetic behaviour" under the influence of a magnetic field, and a transition between the nonmagnetic and/or low magnetic moment state and high magnetic moment state occurs. The metamagnetic transition is related to the itinerant nature of the X atom in the magnetic field. However, in the compounds with magnetic R, ions the 3d band splitting necessary for the formation of a (Co, Fe) magnetic moments can be provided by a molecular field acting from the R magnetic sublattice. The external magnetic field in this case can induce the metamagnetic transition at much lower magnetic fields by assisting the formation of a (Co, Fe) moments.

Various experimental and theoretical studies have been conducted so far to investigate different properties of both $TbCo_2$ and $TbFe_2$ compounds, including the neutron-dependent diffraction powder temperature, the magnetization measurements, the phase transitions, the differential scanning calorimetry, and the electronic

* Corresponding author. Laboratory of Physico-Chemitry of Advanced Materials, University Djillali Liabès, Sidi Bel-Abbes, Algeria.
E-mail addresses: lilo.btf@gmail.com, a.bentouaf@univ-chlef.dz (A. Bentouaf).

http://dx.doi.org/10.1016/j.jallcom.2016.08.046
0925-8388/

structure calculations [6–8]. As a matter of fact, the neutron measurement [8] performed on the $TbCo_2$ compound have shown that it still keeps its C15 Laves cubic structure only above the Curie temperature (TC) while rhombohedral distortion appeared below it. On the other side, through the first principle calculations, phase transitions and differential scanning calorimetry studies [7,8] revealed a magnetic transition of the second order in this compound.

In another work, Jun-Ding et al. [9] studied the magnetic properties and magnetocaloric effect in $TbCo_2$ and have calculated the total change of entropy using the relationship of Maxwell. Halder and coworkers [10] measured the magnetocaloric effect and investigated the magnetic behaviour of the $TbCo_{2-x}$ Fe_x near-stage transition by using "dc" magnetization measurements and neutron diffraction. More recently, the correlation between the magnetic properties of the $TbCo_2$ and the synthesis pressure were carried out both experimentally and theoretically by Burzo et al. [11], while Duct et al. [12] studied the influence of the Fe:Co ratio on the magnetization and magnetostriction of $(Tb_{0.27}$ $Dy_{0.73})(Fe_{1-x},Co_x)_2$. Moreover, Ahuja et al. [13] determined the spin magnetic moment in $TbCo_2$ compound at different temperatures ranging from 6 to 250 K by using the Magnetic Compton Scattering (MCS) technique where they studied its electronic and magnetic properties for the low temperature rhombohedral phase by using an accurate first principles technique. In a similar study, the group of Baudele [14] presented a detailed Magnetic X-ray dichroism (MXD) measurement that was systematically performed on various ferromagnetic $REFe_2$ Laves phases compounds (RE: Ce, Gd, Lu).

Finally, Gratz and coworkers [11] demonstrated the influences of spin fluctuations on the physical properties of RCo_2 Laves phases, that include the magnetic susceptibility, the thermal expansion and the transport phenomena, while Kiyoshi et al. [15] investigated and compared the hydrogen pressure dependence on the structural changes of C15 Laves phase of TbM_2 (M = Fe, Co and Ni) in order to determine the conditions and the mechanism of hydrogen induced amorphization (HIA) of these compounds.

To the best of our knowledge, no detailed theoretical study have been yet performed on the $TbCo_2$ and $TbFe_2$ compounds which constitutes the main focus of our paper, which reports on the theoretical investigation of the structural, electronic, magnetic and elastic properties of the cubic $MgCu_2$-type binary Laves phases $TbCo_2$ and $TbFe_2$ compounds. After briefly describing the computational techniques employed in this study, the result and discussions are presented together with the summary of the main findings and conclusions.

2. Method of calculations

We have used the all electrons full-potential linearized augmented plane waves (FP-LAPW) within the density functional theory (DFT) [16,17] basis set and method [18] as implemented in the WIEN2k code [19–21]. For the exchange-correlation functional, we have used the generalized gradient approximation GGA [22] and GGA+U (U-Hubbard Hamiltonian) [23,24] beyond the local density approximation as proposed by Perdew et al. [24]. For oxides and other highly correlated compounds, local density approximation (LDA) [21] and GGA are known to fail to give the correct ground state. In these systems, the electrons are highly localized. The Coulomb repulsion between the electrons in open shells should be taken into account. As there is no exchange correlation functional that can include this in an orbital independent way, a simpler approach is to add the Hubbard-like on-site repulsion to the Kohn-Sham Hamiltonian. This is known as a LDA + U or GGA+U calculations [25]. The GGA+U method usually reproduces correctly the relative energetic, magnetic ground states, and electronic structure for compounds systems in which GGA habitually fails [26,27].

There are different ways in which this can be implemented. In our work, we have used the method of Anisimov et al. [28] and Liechtenstein et al. [29] where the Coulomb (U) and exchange (J) parameters are used.

In this study, the 4f electrons of the Tb and 3d orbitals of the Co and Fe were treated using the GGA+U approach [27,30,31]. Among the various calculated U values we have tested, the best ones which are in good agreement with the experimental results are 9.46 eV, J = 1.25 eV [32] for Tb, 7.8 eV, J = 8.92 eV for Co and 6.8 eV, J = 0.89 eV for Fe [33]. We should emphasize, that for strongly correlated electron materials, the failure of the standard DFT can also be overcome by other approaches that go beyond DFT such as the hybrid functionals (computationally expensive). The hybrid functionals involve the DFT correlation and a mixing of the local or semi-local DFT exchange with the non-local Hartree–Fock (HF) exchange in a certain proportion to reduce the self-interaction error of DFT. In fact, it is reported that the hybrid functional, such as HSE06 functional, can be used to describe the bands of nonbonding Ln 4f electrons correctly [34,35].

The satisfactory degree of convergence was achieved by considering a number of FP-LAPW basis function up to $R_{MT}K_{max} = 8$, where R_{MT} is the smallest radius of the muffin-tin spheres and the K_{max} is the plane wave cut-off, i.e. the maximum value of the wave vector $K = k + G$, and the maximum length of G for expanding the interstitial density and potential. R_{MT} for Tb, Fe, and Co are 2.2, 1.8, and 1.8 (a.u), respectively. Within the spheres, the charge density and potential are expanded -in terms of crystal harmonics- up to angular momenta $L_{max} = 10$, and a plane wave is used in the interstitial region. The value of the magnitude of the largest vector in charge density Fourier expansion $G_{max} = 12$.

To ensure the convergence of all the calculations, we also tested the Monkhorst-Pack (MP) meshes of the reciprocal lattice space integration and we found that the special k-points should be performed using 47 special k-points in the Brillouin zone for the two compounds under study [36]. The cut-off energy, which defines the separation of valence and core states, was chosen as −6 Ry. We also selected the charge convergence as 0.0001e during self-consistency cycles.

3. Result and discussions

3.1. Structural properties

The $TbCo_2$ and $TbFe_2$ Laves phase has an ordered C15-type structure with space group 227 (*Fd-3m*). The Tb atoms occupy the tetrahedral 8a Wyckoff site (1/8,1/8,1/8) and the Co atoms occupy the octahedral 16d site (1/2,1/2,1/2), as displayed in Fig. 1. The structural properties are obtained by the minimization of the total energy depending on the volumes of $TbCo_2$ and $TbFe_2$ within GGA and GGA+U methods. We have computed the lattice constants, the bulk moduli and the first pressure derivatives of the bulk moduli by fitting the total energy with respect to the volume according to the Murnaghan's equation of state [37]:

$$E_T(V) = \frac{B_0 V}{B_0'}\left[\frac{(V_0/V)^{B_0'}}{B_0' - 1} + 1\right] + E_0 - \frac{V_0 B_0}{B_0' - 1} \quad (1)$$

where B_0 is the bulk modulus, B_0 is the bulk modulus derivative and V_0 is the equilibrium volume. The obtained results are listed in Table 1, and are in good agreement with the experimental calculated values obtained in Refs. [38,39]. However, it's worth noting here that the lattice parameter (a_0) tend to increase when we use the GGA+U approach, while the bulk modulus (B) decreases as a

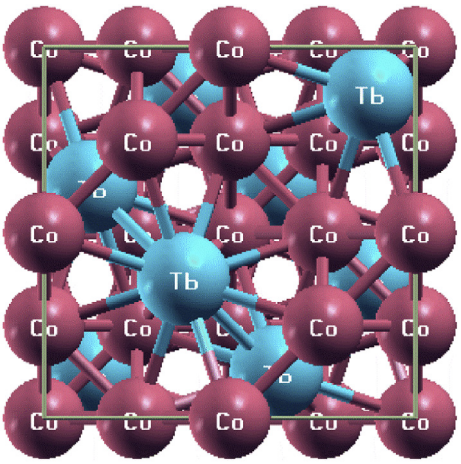

Fig. 1. Schematic of unit cell structure of the $TbCo_2$ intermetallic compounds, the same for the unit cell structure of $TbFe_2$ except we replace Co by Fe.

Table 1
Equilibrium parameters of the $TbCo_2$ and $TbFe_2$: lattice constant a, bulk modulus B.

X	Lattice parameter a (A°)		Bulk modulus B (GPa)
	Our work	Other work	Our work
$TbCo_2$			
GGA	6.985	7.211[a]	129.187
GGA+U	7.40		55.86
$TbFe_2$			
GGA	7.04	7.341[b]	121.033
GGA+U	7.45		81.08

[a] Ref. [38].
[b] Ref. [39].

consequence of its inverse proportionality to the lattice constant. Fig. 2 displays the total energies in dependence on cell volume for both $TbCo_2$ and $TbFe_2$ compounds.

3.2. Electronic properties

Fig. 3 shows the computed spin-polarized band structures for the $TbCo_2$ and $TbFe_2$ at the calculated equilibrium lattice constants along the high symmetry directions W(1/2,1/4,3/4), L(1/2,1/2,1/2), Γ(0,0,0), X(1/2,0,1/2) and K(3/8,3/8,3/4) in the first Brillouin zone (Fig. 2e), by using GGA and GGA+U methods. It is clear that the valence and conduction bands are overlapping around Fermi level. Moreover, there is no band gap at the Fermi level which is clearly indicating that these two compounds (i.e., $TbCo_2$ and $TbFe_2$) are neither insulator nor semiconductor materials but rather conductor ones. In order to elucidate the major contribution of orbit in the band structure and bonding characteristics, the total and partial densities of state (TDOS and PDOS, respectively) of these two compounds are calculated and presented in Fig. 4. By employing the GGA and GGA+U, the spin-up and spin-down TDOS of these two compounds are found to be anti-symmetric, which is indicating that they are in a ferromagnetic state. These results should be attributed to the contribution of 3d states of cobalt (Co) and iron (Fe) atoms and to the contribution of the 4f states of terbium (Tb) as well to the TDOS. In addition, the energy dispersion spectrum is found to cross the Fermi level ($E_F = 0$ eV), which is another indication implying that these compounds are indeed electrically conductor. On the other hand, for the two compounds under study, the low-energy region which is located around −25 and −20 eV is mostly filled by the p states of the Tb atoms, and the major part of the total DOS (from −5 to + 5 eV) is mainly governed by the 3d states of Co and Fe, and by the 4f states of Tb. It has been noticed that the Tb-4f state show the highest contribution among the others.

Fig. 4 summarizes the total densities of states obtained by GGA and GGA+U for the $TbCo_2$ and the $TbFe_2$, respectively. It's well known that one of the main advantages of the GGA+U method is its ability to treat simultaneously delocalized conduction band electrons and localized 3d and 4f electrons states in the same computational scheme. We have applied Hubbard U parameter to slightly push up the higher empty 3d and 4f states to the conduction band. Therefore, the use of GGA+U approach is motivated by the presence of the very localized 4f and delocalized 3d in $TbCo_2$ and $TbFe_2$, respectively.

The DOS at Fermi energy (E_F) is determined by the overlap between the valence and conduction bands. This overlap is strong enough indicating metallic origin with different values of DOS at E_F, $N(E_F)$ (Table 2). The electronic specific heat coefficient (γ), which is function of density of states, can be calculated using the expression,

$$\gamma = \frac{1}{3}\pi^2 N(E_F) k_B^2, \tag{2}$$

here $N(E_F)$, is the density of states at Fermi energy, and k_B is the Boltzmann constant. The calculated density of states at Fermi

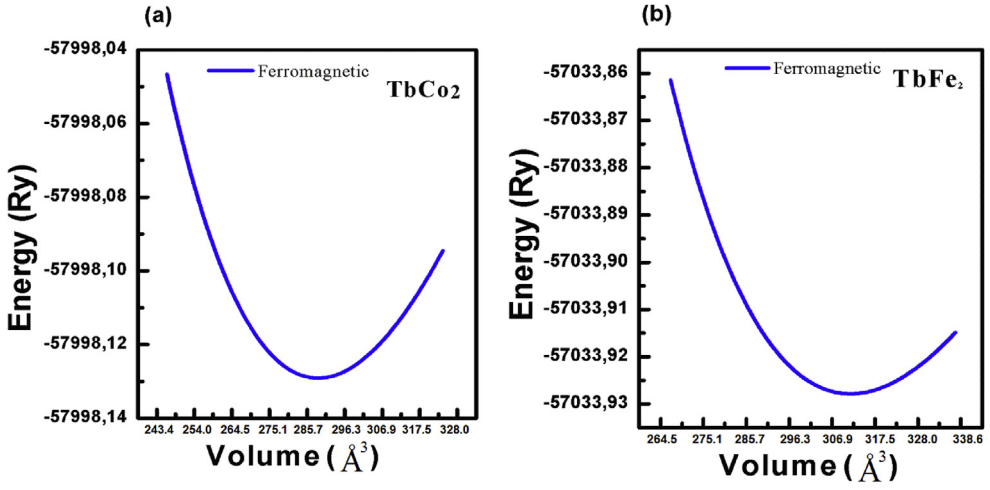

Fig. 2. The total energy E_{tot} of the compounds studied as a function of the volume with GGA calculation adjusting by Murnaghan equation.

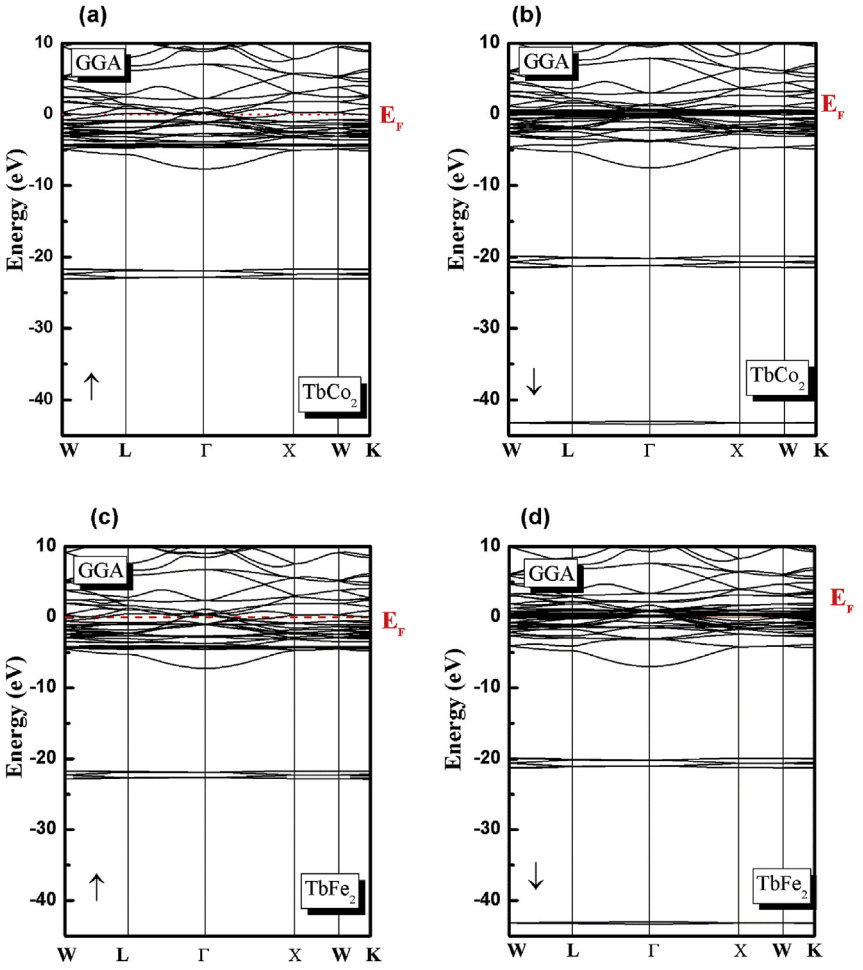

Fig. 3. The calculated band structure of the $TbCo_2$ and $TbFe_2$ as obtained within the **(a–d)** GGA for spin-up and spin-down.

energy $N(E_F)$, enables us to calculate the bare electronic specific heat coefficient (Table 1). To obtain further insight into the type of states associated with each orbital, Fig. 5b,d and Fig. 6b,d shows the projected density of states (DOS) of the Co-d and Fe-d orbitals calculated using GGA and GGA+U, respectively. Careful looking at the orbital decomposed density of states, the highest occupied and lowest unoccupied orbital states for $TbFe_2$ and $TbCo_2$ compounds are found to be Fe-3d-t_{2g} and Co-3d-t_{2g} states.

3.3. Magnetic properties

Table 3 summarizes the calculated total and local magnetic moments per atom within the muffin-tin spheres of $TbCo_2$ and $TbFe_2$, respectively, by using the GGA and GGA+U methods. In the majority of the studied cases, the calculated magnetic moments of the $TbCo_2$ are found to be in good agreement with the experimental results obtained by neutron powder diffraction study [6] and/or by the spin-polarized Compton profiles method [13]. It is well known that the source of magnetic moments in Co and Fe elements are the 3d states. It is clear that the GGA+U gives higher values than that obtained by GGA. The calculated total magnetic moment of $TbCo_2$ is found to be 15.69 (19.25) μB per unit cell, using GGA(GGA+U) while for $TbFe_2$ it is about 18.02 (24.52) μB per unit cell, using GGA(GGA+U). Therefore, the magnetic moment is mostly located in the Tb atom for both the $TbCo_2$ and $TbFe_2$. It should be noted as well that the calculation of the M_{tot} - which is the total spin magnetic moment of the compound- is performed by the integration over the entire cell. Consequently, it is not only the combination of the moments at the Co and Fe (2 times) Tb sites, but also that of the moment related to interstitial between these sites. As a matter of fact, by using the GGA+U, we see that the magnetic moments clearly increase, due to the energy shift of the partial densities of Co, Fe and Tb because of the electron -electron correlation.

3.4. Elastic properties

The mechanical stability of the $TbCo_2$ and $TbFe_2$ compounds was investigated through the calculation of their elastic constants C_{ij}. These constants are necessary to describe the mechanical properties of materials as they are closely related to different fundamental solid-state phenomena, including the interatomic bonding, the equations of state, and the phonon spectra. The elastic constants C_{ij} are obtained by calculating the total energy as a function of the volume conserving strains using the Mehl method [40]. The macroscopic stability of the materials (i.e., stable phases) depends mainly on the positive definiteness of the stiffness matrix [41]. The following conditions, known as the Born Huang criteria [42], are defined as: $C_{11} > 0$, $C_{44} > 0$, $C_{11} > C_{12}$, $(C_{11} + 2C_{12}) > 0$ for the cubic structure. The elastic constants C_{ij} are estimated from the first-principles calculations for $TbCo_2$ and $TbFe_2$ compounds. We have also calculated the shear modulus G, the Young's modulus E, the Poisson's ratio ν, and shear anisotropic factor, which are the elastic moduli for the polycrystalline species, using the following standard relations [43–45]:

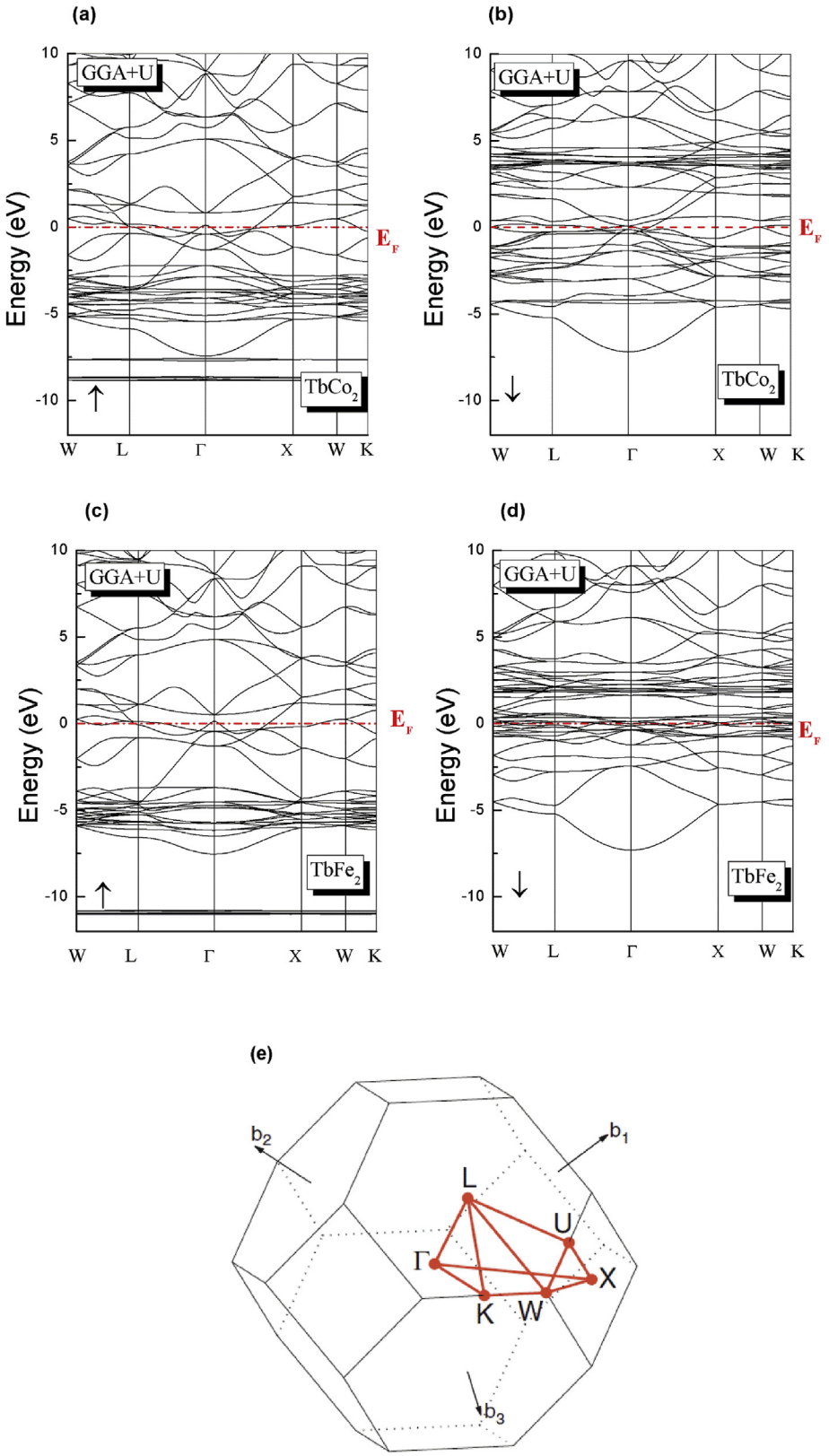

Fig. 4. The calculated band structure of the $TbCo_2$ and $TbFe_2$ as obtained within **(a–d)** GGA+U for spin-up and spin-down; **(e)** Brillouin zone of FCC lattice. Path: W (1/2 1/4 3/4), L (1/2 1/2 1/2), Γ(0 0 0), X (1/2 0 1/2) and K (3/8 3/8 3/4).

Table 2
The density of states at Fermi energy $N(E_F)$ states/Ry cell and the bare electronic specific heat coefficient γ(mJ/mole-K^2).

	$TbCo_2$-up		$TbCo_2$-down		$TbFe_2$-up		$TbFe_2$-down	
	GGA	GGA+U	GGA	GGA+U	GGA	GGA+U	GGA	GGA+U
$N(E_F)$	3.6	4.5	23.5	3.7	3.4	4.1	21.1	14.2
γ	0.62	0.78	4.07	0.64	0.58	0.71	3.66	2.46

$$G = \frac{C_{11} - C_{12} + 3C_{44}}{5} \tag{3}$$

$$E = \frac{9BG}{3B + G} \tag{4}$$

$$\nu = \frac{3B - 2G}{2(3B + G)} \tag{5}$$

$$A = \frac{2C_{44}}{C_{11} - C_{12}} \tag{6}$$

The elastic constants and elastic moduli for polycrystalline materials are calculated within the GGA approximation and are summarized in Table 4.

According to the criteria of stability, we have found that $TbCo_2$ and $TbFe_2$ compounds are mechanically stable against any elastic

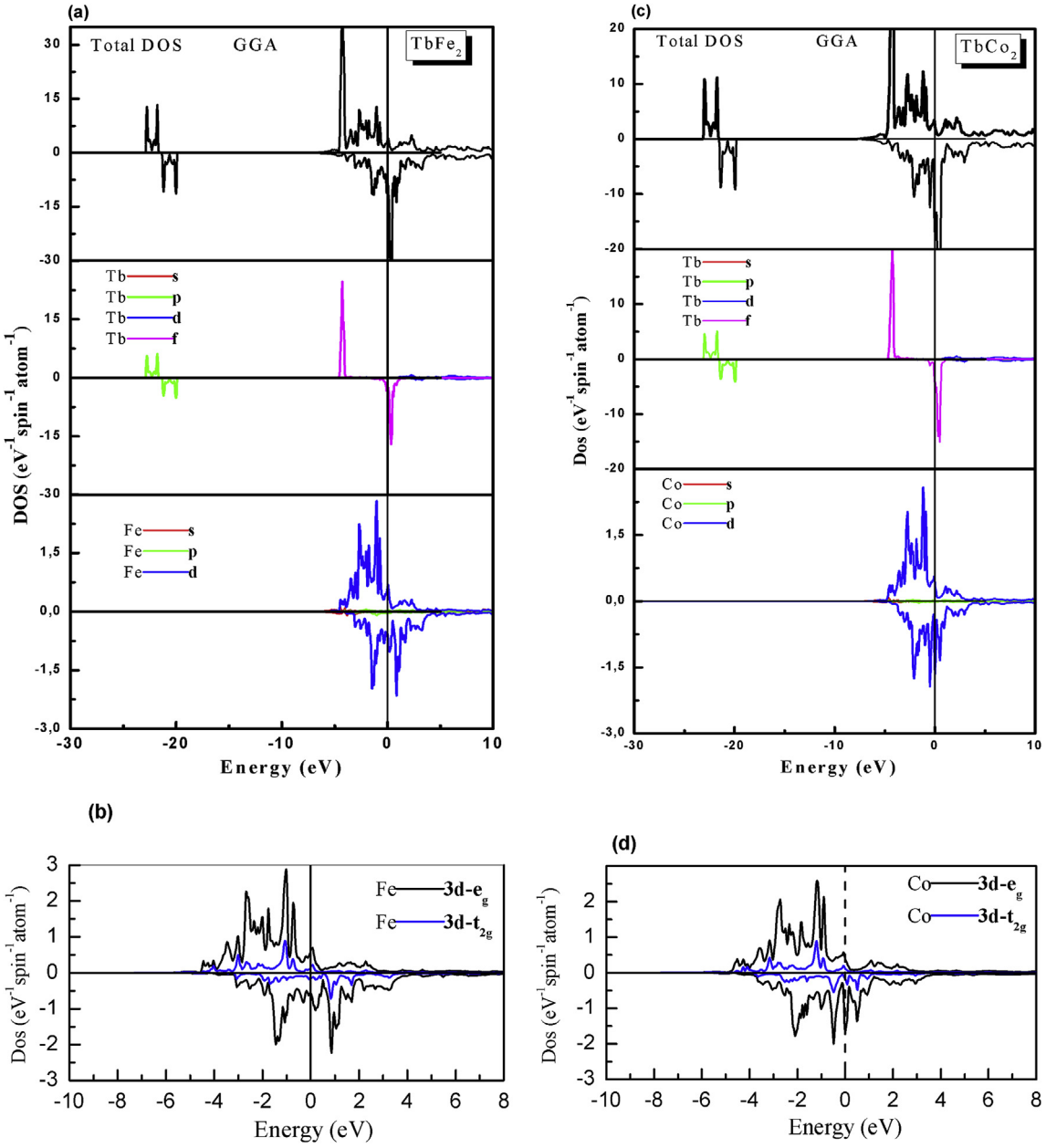

Fig. 5. **(a)** The calculated spin-projected total and partial DOS plots for $TbFe_2$ compound as obtained within GGA; **(b)** The projected density of states (DOS) of the Fe-3d orbitals calculated using GGA; **(c)** The calculated spin-projected total and partial DOS plots for $TbCo_2$ compound as obtained within GGA; **(d)** The projected density of states (DOS) of the Co-3d orbitals calculated using GGA.

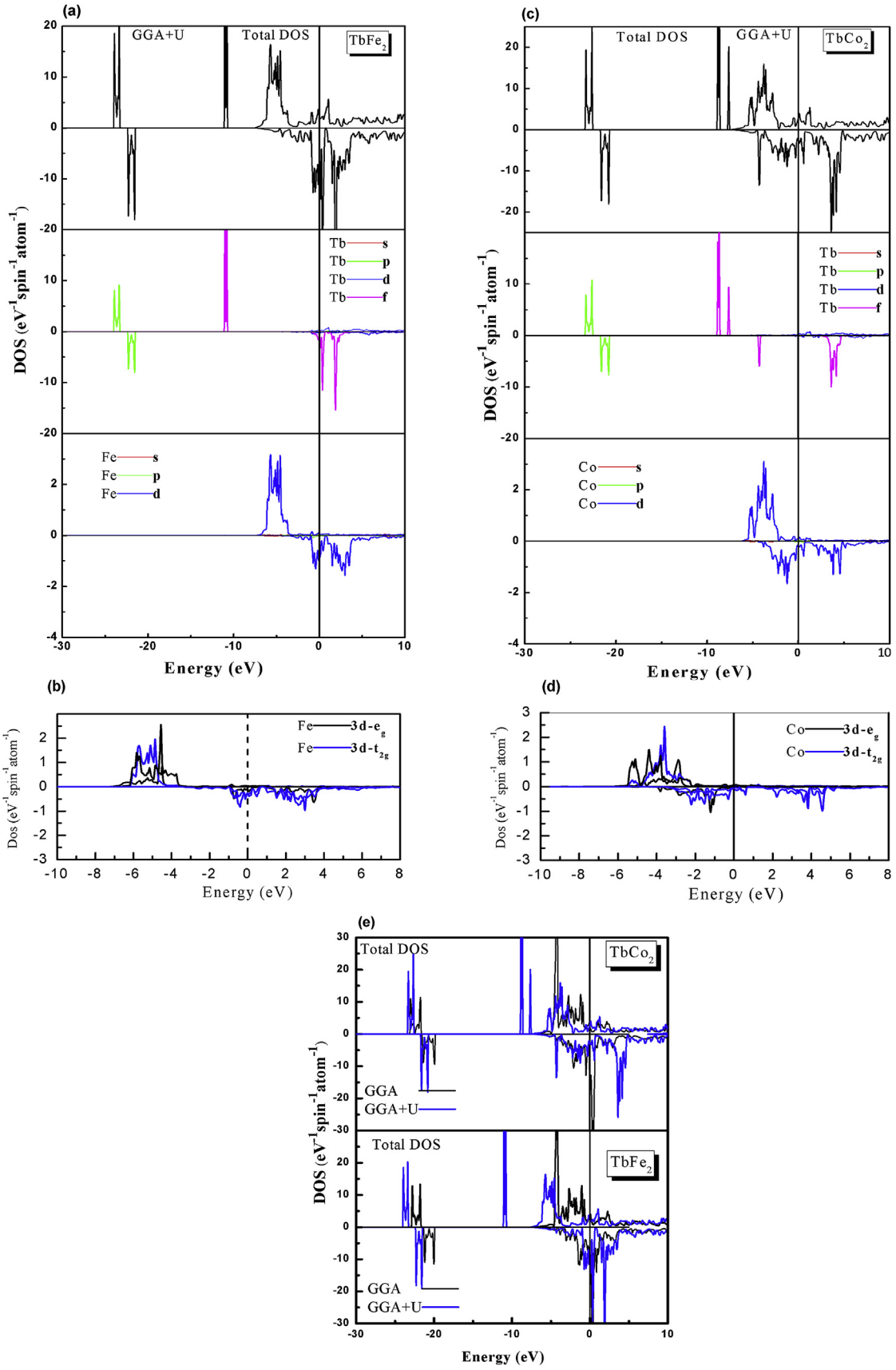

Fig. 6. **(a)** The calculated spin-projected total and partial DOS plots for $TbFe_2$ compound as obtained within GGA+U; **(b)** The projected density of states (DOS) of the Fe-3d orbitals calculated using GGA+U; **(c)** The calculated spin-projected total and partial DOS plots for $TbCo_2$ compound as obtained within GGA+U; **(d)** The projected density of states (DOS) of the Co-3d orbitals calculated using GGA+U; **(e)** Comparison between the calculated spin-projected total DOS obtained by GGA and GGA+U.

Table 3
The calculated total and partial magnetic moments of the $TbCo_2$ and $TbFe_2$ compounds.

$TbCo_2$		M_{tot}	M_{Tb}	M_{Co}	M_{int}
Our work	GGA	15.69	5.82	1.07	−0.24
	GGA+U	19.25	5.90	1.85	0.03
Exp		–	6.33[a], 6.00[b]	1.08[a], −2.04[b]	–
Other work		4.28[b]	6.22[b]	−2.49[b]	0.44[b]
$TbFe_2$		M_{tot}	M_{Tb}	M_{Fe}	M_{int}
Our work	GGA	18.02	5.81	1.69	−0.37
	GGA+U	24.52	6.17	3.26	−0.90

[a] Ref. [36].
[b] Ref. [13].

Table 4
The calculated single crystal elastic constants Cij (in GPa) and polycrystalline elastic modulus (shear modulus G (in GPa), Young's modulus E (in GPa), Poisson's ratio (ν) shear anisotropic factor for $TbCo_2$ and $TbFe_2$ compounds.

	C_{11}	C_{12}	C_{44}	G	E	ν	A
$TbCo_2$	198.00	104.23	77.68	63.44	126.11	0.345	0.312
$TbFe_2$	196.72	112.12	84.26	63.90	115.31	0.363	0.593

deformation. The Cauchy pressure ($pc = C_{12} - C_{44}$) [46,47] is found to be positive, which is a clear indication of a ductile nature. The C_{11} values related to the unidirectional compression along the principal crystallographic direction, is found to be much greater than that of C_{44}, indicating a weak resistance to the shear deformation in comparison to the resistance to the unidirectional compression. Moreover, we have noted that the higher bulk modulus and Young's modulus are suggesting rather a strong incompressibility for both compounds. Also, the calculated values of the Poisson's ratio for the $TbCo_2$ and $TbFe_2$ compounds are found to be more than 0.25, indicating then a metallic contribution in the inter-atomic bounding (To note that the typical value of Poisson's ratio (ν) for ionic materials is 0.25 [48]). For an isotropic crystal, the factor A must be equal to one, while any value different than unity is a measure of elastic anisotropy degree possessed by the crystal [49]. Indeed, our calculated values are somehow relatively deviant from the unity, which means that $TbCo_2$ and $TbFe_2$ compounds should have a lower anisotropy and possesses a low probability to develop microcracks and/or structural defects during their growing process.

4. Conclusions

We have successfully performed a first principle calculation based on the FP-LAPW method within the GGA and GGA+U in order to investigate the electronic, magnetic and elastic properties of the ferromagnetic cubic $MgCu_2$-type binary Laves phases $TbCo_2$ and $TbFe_2$ intermetallic materials. The comparison of the optimized lattice parameters with previous studies has shown that the calculated values corroborated efficiently the experimental values. We have then studied the correlation effects on the electronic properties where we pointed out that when the on-site Coulomb interaction is induced by the GGA+U, the magnetic moments increased. This increase was explained in terms of the energy shift of the partial densities of Co, Fe and Tb by the electron-electron correlation in the GGA+ U calculation. Finally, this model (GGA+U) was found to require a strong interaction (high U) to obtain a qualitative agreement with experimental values, such as behaviour states d, f and the magnetic moments. Furthermore, in order to obtain further insight into the type of states associated with each orbital, the projected DOS of Co-3d and Fe-3d orbitals were calculated using GGA and GGA+U.

Acknowledgements

We acknowledge financial and technical supports from the University Djillali Liabès, at Sidi Bel-Abbes, and the university of Hassiba Ben Bouali, Chlef, Algeria. A. H. R. would like to acknowledge CENTEM project, CZ.1.05/2.1.00/03.0088, co-funded by the ERDF as part of MSMT- OP RDI program and supported through CENTEM PLUS (LO1402) by financial means from MSMT under National Sustainability Program I, MetaCentrum (LM2010005) and CERIT-SC (CZ.1.05/3.2.00/08.0144) infrastructures. B.A. would like to acknowledge the support of the Qatar Energy and Environment Research Institute (QEERI), Hamad Bin Khalifa University, Qatar Foundation, Education City, Doha, Qatar, and the Centre Énergie, Matériaux et Télécommunications, INRS-ÉMT, University of Quebec, Canada.

References

[1] M.I. Batashevich, H.A. Katori, T. Goto, H. Wada, T. Maeda, T. Mori, M. Shiga, Phys. B 229 (1997) 315.
[2] T. Goto, H.A. Katori, T. Sakakibara, H. Mitamura, K. Fukamichi, K. Murata, J. Appl. Phys. 76 (1994) 6682.
[3] T. Goto, K. Fukamichi, H. Yamada, Phys. B 300 (2001) 67.
[4] S. Khmelevskyi, P. Mohn, J. Phys. Condens. Matter 12 (2000) 9453.
[5] E. Gratz, A.S. Markosyan, J. Phys. Condens. Matter 13 (2001) 385.
[6] Z.W. Ouyang, F.W. Wang, Q. Hang, W.F. Liu, G.Y. Liu, J.W. Lynn, J.K. Liang, G.H. Rao, J. Alloys Comp. 390 (2005) 21.
[7] J. Herrero-Albillos, F. Bartolomé, L.M. García, F. Casanova, A. Labarta, X. Batlle, Phys. Rev. B 73 (2006) 134410.
[8] X.B. Liu, Z. Altounian, J. Phys. Condens. Matter 18 (2006) 5503.
[9] Z. Jun-Ding, S. Bao-Gen, S. Ji-Rong, Chin. Phys. 16 (2007) 3843.
[10] M. Halder, S.M. Yusuf, M.D. Mukadam, K. Shashikala, Phys. Rev. B 81 (2010) 174402.
[11] E. Burzo, P. Vlaic, D.P. Kozlenko, S.E. Kichanov, N.T. Dang, E.V. Lukin, B.N. Savenko, J. Alloys Comp. 551 (2013) 702.
[12] N.H. Duc, K. Mackay, J. Betz, Zs Sarkozi, D. Givord, J. Phys. Condens. Matter 12 (2000) 7957.
[13] B.L. Ahuja, H.S. Mund, Jagrati Sahariya, Alpa Dashora, Madhumita Halder, S.M. Yusuf, M. Itou, Y. Sakurai, J. Alloys Comp. 633 (2015) 430.
[14] F. Baudelet, C. Brouder, E. Dartyg, A. Fontain, J.P. Kappler, G. Krill, Europhys. Lett. 13 (8) (1990) 751.
[15] K. Aoki, K. Mori, T. Masumoto, Mater. Trans. 43 (11) (2002) 2685.
[16] P. Hohenberg, W. Kohn, Phys. Rev. B 136 (1964) 864.
[17] W. Kohn, L.J. Sham, Phys. Rev. 140 (1965) A1133.
[18] J.C. Slater, Adv. Quant. Chem. 1 (1964) 5564.
[19] P. Blaha, K. Schwarz, G.K.H. Madsen, D.J. Kvasnicka, WIEN2K, an Augmented Plane Wave +Local Orbitals Program for Calculating Crystal Properties, Karlheinz Schwarz, Technische Universität, Wien, Austria, 2001, ISBN 3-9501031 1–2, 2001.
[20] P. Blaha, K. Schwarz, P. Sorantin, S.B. Tricky, Comput. Phys. Commun. 59 (1990) 399.
[21] K. Schwarz, P. Blaha, G.K.H. Madsen, Comput. Phys. Commun. 147 (2002) 71.
[22] D.C. Langreth, J.P. Perdew, Phys. Rev. B 21 (1980) 5469.
[23] J.P. Perdew, S. Burke, M. Ernzerhof, Phys. Rev. Lett. 77 (1990) 3865.
[24] J.P. Perdew, S. Burke, Y. Wang, Phys. Rev. B 54 (1996) 16533.
[25] D. Rappoport, N.R.M. Crawford, F. Furche, K. Burke, in: E.I. Solomon, R.B. King, R.A. Scott (Eds.), Computational Inorganic and Bioinorganic Chemistry, Wiley, John & Sons, Inc, Wiley, Chichester. Hoboken, 2009.
[26] G.I. Csonka, J.P. Perdew, A. Ruzsinszky, P.H.T. Philipsen, S. Lebegue, J. Paier, O.A. Vydrov, J.G. Angyan, Phys. Rev. B 79 (2009) 155107.
[27] V.I. Anisimov, J. Zaanen, O.K. Andersen, Phys. Rev. B 44 (1991) 943.

[28] V.I. Anisimov, I.V. Solovyev, M.A. Korotin, M.T. Czyzyk, G.A. Sawatzky, Phys. Rev. B 48 (1993) 16929.
[29] A.I. Liechtenstein, V.I. Anisimov, J. Zaanen, J. Phys. Rev. B 52 (1995) R5467.
[30] V.I. Anisimov, O. Gunnarsson, Phys. Rev. B 43 (1991) 7570.
[31] V.I. Anisimov, I.V. Solovyev, M.A. Korotin, M.T. Czyżyk, G.A. Sawatzky, Phys. Rev. B 48 (1993) 16929.
[32] P. Larson, R.L. Walter, Phys. Rev. B 75 (2007) 045114.
[33] V.I. Anisimov, J. Zaane, O.K. Andersen, Phys. Rev. B 44 (1991) 943.
[34] I.A.M. Ibrahim, Z. Lenčéš, P. Šajgalík, L. Benco, J. Lumin. 164 (2015) 131.
[35] I.A.M. Ibrahim, Z. Lenčéš, L. Benco, P. Šajgalík, J. Lumin. 172 (2016) 83.
[36] H.J. Monkhorst, J.D. Pack, Phys. Rev. B 13 (1976) 5188.
[37] F.D. Murnaghan, Proc. Natl. Acad. Sci. U. S. A. 30 (1944) 244.
[38] V.V. Burnasheva, V.A. Yartys, A.V. Ivanov, K.N. Semenenko, R. J. Inorg. Chem. 24 (1979) 2038.
[39] K.H.J. Buschow, Physica B+C 86–88 (1) (1977) 79–80.
[40] M.J. Mehl, Phys. Rev. B Condens. Matter 47 (1993) 2493–2500.
[41] F.I. Fedoras, Theory of Elastic Waves in Crystals, Oxford University Press, New York, 1985.
[42] M. Born, K. Huang, Dynamical Theory and Experiment I, Springer Verlag, Berlin, 1982.
[43] M.J. Mehl, B.K. Klein, D.A. Papaconstantopoulos, Intermetallic com- pounds: principle and practice, in: J.H. Westbrook, R.L. Fleischeir (Eds.), Principles, I, John Wiley and Sons, 1995.
[44] W. Voigt, Lehrbush der Kristallphysik, Taubner, Leipzig, 1928.
[45] E. Schreiber, O.L. Anderson, N. Soga, Elastic Constants and Their Measurements, McGraw-Hill, New York, NY, 1973.
[46] D.G. Pettifor, Mater. Sci. Technol. 8 (1992) 345.
[47] V. Kanchana, G. Vaitheeswaran, Yanning Ma, Yu Xie, A. Svane, O. Eriksson, Phys. Rev. B 80 (2009) 125108.
[48] J. Haines, J.M. Léger, G. Bocquillon, Annu. Rev. Mater. Res. 31 (2001) 1.
[49] Z. Biskri, H. Rached, M. Bouchear, D. Rached, J. Mech. Behav.. Bio. Mater 32 (2014) 345.